View metadata, citation and similar papers at core.ac.uk

brought to you by CORE

provided by DigitalCommons@University of Nebraska

University of Nebraska - Lincoln
DigitalCommons@University of Nebraska - Lincoln

Faculty Publications from the Department of Electrical and Computer Engineering

Electrical & Computer Engineering, Department of

2011

Terahertz optical-Hall effect characterization of two-dimensional electron gas properties in AlGaN/GaN high electron mobility transistor structures

S. Schöche
University of Nebraska–Lincoln, schoeche@huskers.unl.edu

Junxia Shi
Cornell University

A. Boosalis
University of Nebraska–Lincoln

P. Kühne
University of Nebraska–Lincoln

C. M. Herzinger
J.A. Woollam Co. Inc.

See next page for additional authors

Follow this and additional works at: http://digitalcommons.unl.edu/electricalengineeringfacpub


Part of the Computer Engineering Commons, and the Electrical and Computer Engineering Commons

Schöche, S.; Shi, Junxia; Boosalis, A.; Kühne, P.; Herzinger, C. M.; Woollam, John A.; Schaff, W. J.; Eastman, L. F.; Schubert, M.; and Hofmann, Tino, "Terahertz optical-Hall effect characterization of two-dimensional electron gas properties in AlGaN/GaN high electron mobility transistor structures" (2011). *Faculty Publications from the Department of Electrical and Computer Engineering*. 224.
http://digitalcommons.unl.edu/electricalengineeringfacpub/224

This Article is brought to you for free and open access by the Electrical & Computer Engineering, Department of at DigitalCommons@University of Nebraska - Lincoln. It has been accepted for inclusion in Faculty Publications from the Department of Electrical and Computer Engineering by an authorized administrator of DigitalCommons@University of Nebraska - Lincoln.

Authors
S. Schöche, Junxia Shi, A. Boosalis, P. Kühne, C. M. Herzinger, John A. Woollam, W. J. Schaff, L. F. Eastman, M. Schubert, and Tino Hofmann

This article is available at DigitalCommons@University of Nebraska - Lincoln: http://digitalcommons.unl.edu/electricalengineeringfacpub/224

Terahertz optical-Hall effect characterization of two-dimensional electron gas properties in AlGaN/GaN high electron mobility transistor structures

S. Schöche,[1,a)] Junxia Shi,[2] A. Boosalis,[1] P. Kühne,[1] C. M. Herzinger,[3] J. A. Woollam,[3] W. J. Schaff,[2] L. F. Eastman,[2] M. Schubert,[1] and T. Hofmann[1]
[1]*Department of Electrical Engineering and Nebraska Center for Materials and Nanoscience, University of Nebraska–Lincoln, Lincoln, Nebraska 68588-0511, USA*
[2]*Department of Electrical and Computer Engineering, Cornell University, Ithaca, New York 14853, USA*
[3]*J.A. Woollam Co. Inc., 645 M Street, Suite 102, Lincoln, Nebraska 68508-2243, USA*

(Received 15 December 2010; accepted 29 January 2011; published online 28 February 2011)

The free-charge carrier mobility, sheet density, and effective mass of a two-dimensional electron gas are exemplarily determined in the spectral range from 640 GHz to 1 THz in a AlGaN/GaN heterostructure using the optical-Hall effect at room temperature. Complementary midinfrared spectroscopic ellipsometry measurements are performed for analysis of heterostructure constituents layer thickness, phonon mode, and free-charge carrier parameters. The electron effective mass is determined to be $(0.22 \pm 0.04)m_0$. The high-frequency sheet density and carrier mobility parameters are in good agreement with results from dc electrical Hall effect measurements, indicative for frequency-independent carrier scattering mechanisms of the two-dimensional carrier distribution. © *2011 American Institute of Physics*. [doi:10.1063/1.3556617]

Electronic device structures for gigahertz and terahertz frequency applications and for high-power switches require materials with high breakdown voltages, large charge carrier saturation velocities, and high thermal stability.[1] Such requirements can be met by group-III nitride semiconductor alloys.[1,2] High-frequency, high-power nitride-based high electron mobility transistor (HEMT) structures can be obtained by growth of a thin pseudomorphic AlGaN layer onto a thick unstrained GaN layer, for example. A two-dimensional electron gas (2DEG) then forms at the interface between GaN and AlGaN due to differences of the spontaneous and piezoelectric polarizations of the unstrained GaN layer and the tensile strained AlGaN layer.[3] For optimization of device performance parameters, experimental access to the buried conductive 2DEG channel is required for precise determination of the charge carrier channel parameters mobility, sheet density, and effective mass. For high-frequency applications, in particular for upper gigahertz and future terahertz electronics, evaluation of the 2DEG parameters at the operating frequencies is currently a challenge. The information about the charge carrier properties at high frequencies is highly relevant. In linear Boltzmann transport theory, the charge carriers within the 2DEG are governed by a two-dimensional-momentum energy distribution function. The high-frequency properties may be fundamentally different from dc or low-frequency electrical transport properties, for example due to frequency-dependent carrier scattering mechanisms.[4] Electrical methods require device fabrication and frequency-dependent transport evaluation. Optical methods dispense with the need of electrical contacts and are not limited toward higher frequencies.

We have shown that the optical-Hall effect (OHE), which comprises generalized spectroscopic ellipsometry measurements in combination with external magnetic fields, can be employed at terahertz frequencies.[5–8] The OHE is an excellent tool for noncontact characterization of free-charge carrier properties in semiconductor structures.[9,10] The classical Drude model is sufficient to analyze OHE data, when allowing for magnetic-field dependent free-charge carrier parameters. This approach then provides access to the energy-distribution-averaged free-charge carrier properties at terahertz frequencies. Field-dependent OHE measurements, i.e., at variable magnetic field magnitudes, permit extrapolation to the zero-field effective mass, sheet density, and mobility parameters, if needed. The Boltzmann transport theory then renders these zero-field parameters identical to those responsible for terahertz electric transport in zero magnetic field and which are relevant for device optimization, regardless of the actual energy distribution and band structure properties.[4]

In this work we demonstrate characterization of the 2DEG charge carrier channel parameters in AlGaN/GaN HEMT structures using OHE measurements from 640 GHz to 1 THz (THz-OHE). The high-frequency sheet density and carrier mobility parameters are in good agreement with results from dc electrical-Hall effect measurements, indicative for frequency-independent carrier scattering mechanisms of the two-dimensional carrier distribution in AlGaN/GaN heterostructures. Complementary midinfrared spectroscopic ellipsometry (MIR-SE) measurements are performed for analysis of heterostructure constituents layer thickness, phonon mode, and free-charge carrier parameters.[11]

The sample studied here was grown by metal-organic chemical vapor deposition on a GaN epiready *c*-plane Al_2O_3 substrate (Velox Semiconductor, Somerset, New York). The sample consists of a nominally 1 μm thick GaN buffer layer followed by a 1 nm AlN spacer and a 23 nm thick $Al_{0.26}Ga_{0.74}N$ electron barrier layer. The surface of the $Al_{0.26}Ga_{0.74}N$ layer was passivated by a 15 nm HfO_2 layer, deposited by atomic layer deposition. The electrical properties of the 2DEG formed within the GaN layer can be significantly influenced by surface passivation,[12,13] for example

a)Electronic mail: schoeche@huskers.unl.edu.

 © 2011 American Institute of Physics

with HfO_2.[14,15] The influence of the surface passivation layer properties onto the 2DEG parameters is subject of a forthcoming report. Further information on growth conditions and structural analysis can be found in Ref. 15. The dc electrical-Hall effect measurements were performed in the Van der Pauw geometry at room temperature. The generalized ellipsometry formalism is employed for the terahertz and MIR optical investigations. The optical response of the sample is represented using the Mueller matrix formalism.[16] A custom-built frequency-domain terahertz ellipsometer was used for the THz-OHE measurements in the spectral range from 0.65 to 1.00 THz with a resolution of 1 GHz.[17] The THz-OHE measurements were carried out at an angle of incidence $\Phi_a = 74.5°$. The magnetic field strength was varied between $B = -1.5$ to $+1.5$ T with a field direction oriented perpendicular to the sample surface.[7,17] The MIR-SE measurements have been carried out using a commercial Fourier transform-based MIR ellipsometer (J.A. Woollam Co. Inc., Lincoln, Nebraska) in the spectral range from 10 to 45 THz (333 to 1500 cm^{-1}) with a resolution of 60 GHz (2 cm^{-1}).

The experimental MIR-SE and THz-OHE data sets were combined in a stratified layer model analysis using parameterized model dielectric functions. All model calculated data were matched simultaneously as closely as possible to the experimental MIR-SE and THz-OHE data sets by varying relevant physical model parameters (best-model).[18] The THz and MIR spectral range dielectric functions of the sample constituents consist of contributions from optically active phonon modes $\varepsilon^{L}(\omega)$ and free-charge carrier excitations $\varepsilon^{FC}(\omega)$. The dielectric functions of the nitride layers (wurtzite-structure) and the sapphire substrate (corundum structure) are optically anisotropic (uniaxial). Functions $\varepsilon_j^{L}(\omega)$ are parameterized with Lorentzian lineshapes which account for transverse (TO) and longitudinal optic (LO) phonon frequencies, $\omega_{TO,j}$ and $\omega_{LO,j}$, respectively, for polarization $j = "\parallel", "\perp"$ to the crystal c-axis.[11] $\varepsilon^{FC}(\omega)$ is parameterized using the classical Drude formalism.[19] If magnetic fields are present the free-charge carrier Drude contribution is described by a tensor which allows for determination of the screened plasma frequency tensor $\boldsymbol{\omega}_p$ and the cyclotron frequency tensor $\boldsymbol{\omega}_c$:[9,19]

$$\boldsymbol{\varepsilon}^{FC\text{-}MO}(\omega) = \varepsilon_{DC}\boldsymbol{I} + \boldsymbol{\omega}_p^2 \times \left[-\omega^2 \boldsymbol{I} - i\omega\boldsymbol{\gamma} + i\omega \begin{pmatrix} 0 & b_3 & -b_2 \\ -b_3 & 0 & b_1 \\ b_2 & -b_1 & 0 \end{pmatrix} \boldsymbol{\omega}_c \right]^{-1}. \quad (1)$$

The free-charge carrier mobility tensor is given by $\boldsymbol{\mu} = q/(\boldsymbol{\gamma}\boldsymbol{m}^{\star})$ where $\boldsymbol{m}^*$ denotes the effective mass tensor in units of the free electron mass m_0. $\boldsymbol{\omega}_p$ is related to the free-charge carrier density N and the effective mass tensor $\boldsymbol{m}^*$ by $\boldsymbol{\omega}_p^2 = Nq^2/(\varepsilon_\infty \tilde{\varepsilon}_0 \boldsymbol{m}^* m_0)$, where q denotes the charge, $\tilde{\varepsilon}_0$ is the vacuum permittivity, and ε_∞ denotes the high frequency dielectric constant. The cyclotron frequency tensor is defined as $\boldsymbol{\omega}_c = qB/(m_0)\boldsymbol{m}^{*-1}$. The dc dielectric constant is given by ε_{DC} and $\boldsymbol{I}$ is the identity matrix. The external magnetic field is given by $\boldsymbol{B} = B(b_1, b_2, b_3)$ with $|\boldsymbol{B}| = B$.

For best-match model calculation, a model consisting of Al_2O_3 substrate/GaN buffer layer/GaN HEMT channel/AlN layer/AlGaN layer/HfO_2 layer was implemented. Figure 1 depicts the MIR-SE M_{12}, M_{21}, and M_{33} spectra of the AlGaN/GaN heterostructure obtained at an angle of incidence of $\Phi_a = 70°$. The experimental (dotted lines) and best-model calculated (solid lines) data are found to be in very good agreement. The spectra are dominated by the rest-strahlen band of Al_2O_3 and the GaN buffer layer. The positions of the phonon frequencies are indicated by brackets in Fig. 1. The AlGaN layer imposes subtle features in the spectral range from 16 to 23.5 THz. The phonon frequencies and broadening parameters for the dielectric functions of Al_2O_3 and AlN have been taken from Refs. 20 and 21 and were not further varied during the model analysis. The best-model phonon resonance frequency and broadening parameters for the GaN layer which have been obtained from MIR-SE measurements shown in Fig. 1 are $\omega_{TO,\perp} = (559.6 \pm 0.5)$ cm^{-1}, $\omega_{TO,\perp} = (745.8 \pm 0.5)$ cm^{-1}, $\gamma_\perp = (7.6 \pm 0.1)$ cm^{-1}, $\omega_{TO,\parallel} = 534$ cm^{-1}, $\omega_{LO,\parallel} = (735.1 \pm 0.1)$ cm^{-1}, and $\gamma_\parallel = (5.5 \pm 0.1)$ cm^{-1} and are in good agreement with literature values.[22] The best-model parameters for $Al_{0.26}Ga_{0.74}N$ are $\omega_{TO,\perp}^{AlN} = (637.1 \pm 0.5)$ cm^{-1}, $\omega_{TO,\perp}^{AlN} = 786$ cm^{-1}, $\gamma_{TO,\perp}^{AlN} = (28.6 \pm 0.5)$ cm^{-1}, $\gamma_{LO,\perp}^{AlN} = (2.3 \pm 0.1)$ cm^{-1}, $\omega_{TO,\perp}^{GaN} = (559.8 \pm 0.1)$ cm^{-1}, $\omega_{TO,\perp}^{GaN} = (619.7 \pm 0.5)$ cm^{-1}, $\gamma_{TO,\perp}^{GaN} = (2.3 \pm 0.1)$ cm^{-1}, and $\gamma_{LO,\perp}^{GaN} = (28.6 \pm 0.5)$ cm^{-1} in good agreement with Ref. 21. The parameters for the polarization parallel to the c-axis were not further varied and have been taken from Ref. 21. No phonon signatures have been observed in the MIR-SE data from the amorphous HfO_2 layer for which the optical properties used in the model calculation were extrapolated from NIR ellipsometric measurements.[23]

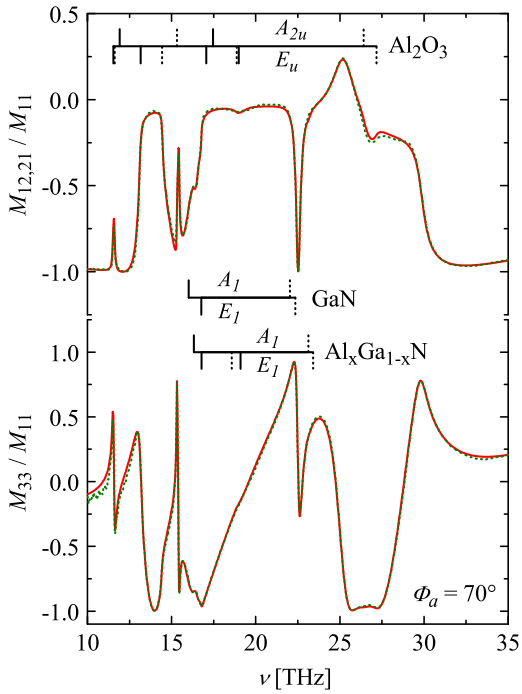

FIG. 1. (Color online) Experimental (dotted lines) and best-model calculated (solid lines) M_{12}, M_{21}, and M_{33} spectra for the HfO_2 passivated AlGaN/GaN HEMT structure in the spectral range from 10 to 45 THz at an angle of incidence $\Phi_a = 70°$. The frequencies of the IR-active phonon modes of the GaN and AlGaN layers and the Al_2O_3 substrate are indicated by brackets (solid: TO; dotted: LO).

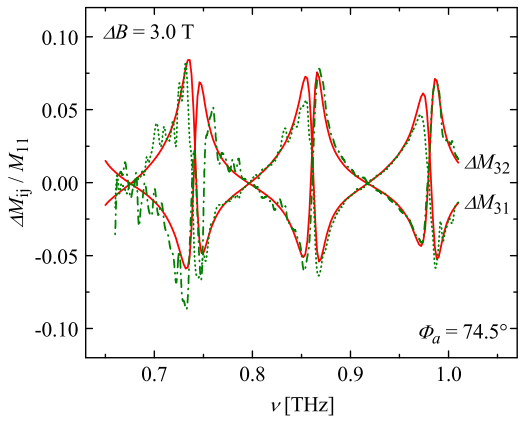

FIG. 2. (Color online) Experimental (dotted lines, ΔM_{31}; dash-dotted lines, ΔM_{32}) and best-model calculated (solid lines) Mueller matrix difference spectra $[\Delta M_{ij}=M_{ij}(B=+1.5\ \mathrm{T})-M_{ij}(B=-1.5\ \mathrm{T})]$ for the HfO_2 passivated AlGaN/GaN HEMT structure in the terahertz frequency domain obtained at an angle of incidence $\Phi_a=74.5°$.

The THz-OHE spectra (differences of the Mueller matrix elements measured at $B=1.5$ and -1.5 T) are presented in Fig. 2. The magnetic field is oriented perpendicular to the sample surface with the sample mounted directly to the magnet's pole face. The THz-OHE data are dominated by Fabry–Pérot interference pattern originating from the complete sample including the Al_2O_3 substrate. The Mueller matrix differences in M_{32} and M_{31} are proportional to percentage of cross-polarization emerging from the sample under linear polarized light illumination at the given frequency.[9,11] Only the free-charge carriers within the high electron mobility 2DEG are responsible for the field and frequency-dependent THz-OHE data. No free-charge carrier contributions were found in the AlGaN electron supplier layer and the AlN spacer as expected from bandstructure considerations. Free-charge carrier contributions from the defect rich interface region between the Al_2O_3 substrate and the GaN buffer layer do not significantly influence the THz-OHE or the MIR-SE data. The frequency of the Fabry–Pérot interference pattern is determined by the layer thicknesses of all sample constituents, dominated by the thickness of the substrate (421.7 ± 0.8) μm. All other layer thicknesses are obtained from the MIR-SE analysis and are in good agreement with the nominal values. The optical response of the GaN HEMT channel was implemented using Eq. (1). When obtaining sheet density parameters N_s, the model thickness parameter for each layer cancels out mathematically within the ellipsometric equations for layers with thickness parameters much smaller than the wavelengths, and is irrelevant for data analysis. The best-match between experimental and model calculated data reveals a n-type channel toward the substrate with sheet carrier density $N_s=(5\pm2)\times10^{12}$ cm^{-2}, mobility $\mu=(1459\pm200)$ cm^2 V^{-1} s^{-1}, and effective mass $(0.22\pm0.04)m_0$ parameters. The electrical-Hall effect measurements resulted in $\mu=(1700\pm50)$ cm^2 V^{-1} s^{-1} and $N_s=(9.9\pm0.3)\times10^{12}$ cm^{-2}. These values agree well with the THz-OHE results. The high-frequency sheet density and carrier mobility parameters are in good agreement with results from dc electrical-Hall effect measurements. The agreement between both parameter sets may be interpreted within linear Boltzmann transport theory by frequency-independent scatter mechanisms within the two-dimensional-momentum energy distribution function of the 2DEG in AlGaN/GaN heterostructures.

In summary, we have determined AlGaN/GaN 2DEG mobility, sheet density, and effective mass parameters at terahertz frequencies, and compared with dc electrical-Hall effect results. Both parameter sets are in good agreement, indicative for frequency-independent carrier scattering mechanisms within the 2DEG energy distribution function.

The authors would like to acknowledge financial support from the Army Research Office (D. Woolard, Contract No. W911NF-09-C-0097), the National Science Foundation (Grant Nos. MRSEC DMR-0820521, MRI DMR-0922937, and DMR-0907475), the University of Nebraska–Lincoln, and the J.A. Woollam Foundation.

[1]L. F. Eastman, V. Tilak, J. Smart, B. M. Green, E. M. Chumbes, R. Dimitrov, H. Kim, O. S. Ambacher, N. Weimann, T. Prunty, M. Murphy, W. J. Schaff, and J. R. Shealy, IEEE Trans. Electron Devices **48**, 479 (2001).
[2]Y.-F. Wu, D. Kapolnek, J. P. Ibbetson, P. Parikh, B. P. Keller, and U. K. Mishra, IEEE Trans. Electron Devices **48**, 586 (2001).
[3]O. S. Ambacher, J. Smart, J. R. Shealy, N. G. Weimann, K. Chu, M. Murphy, W. J. Schaff, L. F. Eastman, R. Dimitrov, L. Wittmer, M. Stutzmann, W. Rieger, and J. Hilsenbeck, J. Appl. Phys. **85**, 3222 (1999).
[4]C. M. Wolfe, N. Holonyak, and G. E. Stillmann, *Physical Properties of Semicoductors* (Prentice-Hall, Englewood Cliffs, NJ, 1989).
[5]Y. Ino, R. Shimano, Y. Svirko, and M. Kuwata-Gonokami, Phys. Rev. B **70**, 155101 (2004).
[6]O. Morikawa, A. Quema, S. Nashima, H. Sumikura, T. Nagashima, and M. Hangyo, J. Appl. Phys. **100**, 033105 (2006).
[7]T. Hofmann, C. M. Herzinger, J. L. Tedesco, D. K. Gaskill, J. A. Woollam, and M. Schubert, "Terahertz ellipsometry and terahertz optical-Hall effect," Thin Solid Films (in press).
[8]T. Hofmann, A. Boosalis, P. Kühne, C. M. Herzinger, J. A. Woollam, D. K. Gaskill, J. L. Tedesco, and M. Schubert, Appl. Phys. Lett. **98**, 041906 (2011).
[9]T. Hofmann, C. M. Herzinger, and M. Schubert, Phys. Status Solidi A **205**, 779 (2008).
[10]M. Schubert, T. Hofmann, and C. M. Herzinger, J. Opt. Soc. Am. A **20**, 347 (2003).
[11]M. Schubert, *Infrared Ellipsometry on Semiconductor Layer Structures: Phonons, Plasmons, and Polaritons*, Springer Tracts in Modern Physics Vol. 209 (Springer, Berlin, 2004).
[12]B. M. Green, K. K. Chu, E. M. Chumbes, J. A. Smart, J. R. Shealy, and L. F. Eastman, IEEE Electron Device Lett. **21**, 268 (2000).
[13]R. Vetury, N. Q. Zhang, S. Keller, and U. K. Mishra, IEEE Trans. Electron Devices **48**, 560 (2001).
[14]J. Shi, L. F. Eastman, X. Xin, and M. Pophristic, Appl. Phys. Lett. **95**, 042103 (2009).
[15]J. Shi and L. F. Eastman, IEEE Electron Device Lett. **32**(3), 312 (2011).
[16]H. Fujiwara, *Spectroscopic Ellipsometry* (Wiley, New York, 2007).
[17]T. Hofmann, C. M. Herzinger, A. Boosalis, T. E. Tiwald, J. A. Woollam, and M. Schubert, Rev. Sci. Instrum. **81**, 023101 (2010).
[18]G. E. Jellison, Thin Solid Films **313–314**, 33 (1998).
[19]C. R. Pidgeon, in *Handbook on Semiconductors*, edited by M. Balkanski (North-Holland, Amsterdam, 1980).
[20]M. Schubert, T. E. Tiwald, and C. M. Herzinger, Phys. Rev. B **61**, 8187 (2000).
[21]M. Schubert, A. Kasic, T. E. Tiwald, J. Off, B. Kuhn, and F. Scholz, MRS Internet J. Nitride Semicond. Res. **4**, 11 (1999).
[22]A. Kasic, M. Schubert, S. Einfeldt, D. Hommel, and T. E. Tiwald, Phys. Rev. B **62**, 7365 (2000).
[23]J. M. Khoshman and M. E. Kordesch, Surf. Coat. Technol. **201**, 3530 (2006).